

1 **Adding gene transcripts into genomic prediction improves accuracy and reveals**
2 **sampling time dependence**

3 B.C. Perez¹, M.C.A.M. Bink¹, K.L. Svenson², G.A. Churchill², M.P.L. Calus^{3*}

4 ¹*Hendrix Genetics B.V., Research and Technology Center (RTC), P.O. Box 114, 5830 AC*
5 *Boxmeer, the Netherlands.*

6 ²*The Jackson Laboratory, Bar Harbor, Maine, United States of America.*

7 ³*Wageningen University & Research, Animal Breeding and Genomics, P.O. Box 338, 6700*
8 *AH Wageningen, the Netherlands.*

9

10 *Corresponding author: mario.calus@wur.nl *Wageningen University & Research, Animal*
11 *Breeding and Genomics, P.O. Box 338, 6700 AH Wageningen, the Netherlands*

12

13 Running title: Transcriptomic prediction accuracy

14

15 **ABSTRACT**

16 Recent developments allowed generating multiple high quality 'omics' data that could increase
17 predictive performance of genomic prediction for phenotypes and genetic merit in animals and
18 plants. Here we have assessed the performance of parametric and non-parametric models
19 that leverage transcriptomics in genomic prediction for 13 complex traits recorded in 478
20 animals from an outbred mouse population. Parametric models were implemented using best
21 linear unbiased prediction (BLUP), while non-parametric models were implemented using the
22 gradient boosting machine algorithm (GBM). We also propose a new model named GTCBLUP
23 that aims to remove between-omics-layer covariance from predictors, whereas its counterpart
24 GTBLUP does not do that. While GBM models captured more phenotypic variation, their
25 predictive performance did not exceed the BLUP models for most traits. Models leveraging
26 gene transcripts captured higher proportions of the phenotypic variance for almost all traits
27 when these were measured closer to the moment of measuring gene transcripts in the liver.
28 In most cases, the combination of layers was not able to outperform the best single-omics
29 models to predict phenotypes. Using only gene transcripts, the GBM model was able to
30 outperform BLUP for most traits except body weight, but the same pattern was not observed
31 when using both SNP genotypes and gene transcripts. Although the GTCBLUP model was
32 not able to produce the most accurate phenotypic predictions, it showed highest accuracies
33 for breeding values for 9 out of 13 traits. We recommend using the GTBLUP model for
34 prediction of phenotypes and using the GTCBLUP for prediction of breeding values.

35

36 **INTRODUCTION**

37 Predicting complex traits is a fundamental aim of quantitative genetics. The use of
38 whole genome single nucleotide polymorphisms (SNP) revolutionized the prediction of
39 breeding values, resulting in the process widely known as genomic prediction (GP)
40 (Meuwissen *et al.* 2001). A number of statistical approaches are now applied routinely in
41 breeding programs, such as genomic best linear unbiased prediction (GBLUP) (VanRaden
42 2008), ridge regression (Whittaker *et al.* 2000), or methods from the “Bayesian Alphabet”
43 (Gianola *et al.* 2009). More recently, machine learning algorithms have been tested in the
44 context of genomic prediction (González-Recio *et al.* 2013; Pook *et al.* 2020; Zingaretti *et al.*
45 2020). These models may have several advantages when compared to traditional linear
46 models, such as capturing interactions between predictors (non-additive effects), automatic
47 variable selection and for making fewer assumptions regarding the underlying genetic
48 architecture of phenotypes (Nayeri *et al.* 2019; Pérez-Enciso and Zingaretti 2019). However,
49 compared to the linear models mentioned above, prediction performance from machine
50 learning methods has shown mixed results (Azodi *et al.* 2019; Abdollahi-Arpanahi *et al.* 2020;
51 Perez *et al.* 2022). There seems to be no “one-size-fits-all” model, as results are dependent
52 on trait genetic architecture, size of the data, and on fine tuning of hyperparameters.

53 Recent development of low-cost high throughput molecular technologies allowed
54 generating multiple high quality ‘omics’ data can be measured with high accuracy (Fernie and
55 Schauer 2009; Tohge and Fernie 2015; Chawade *et al.* 2016). This has led to interest in
56 utilizing these as new layers of information to improve the predictive performance of genomic
57 prediction models, ultimately contributing to improve efficiency of breeding programs (Guo *et*
58 *al.* 2016; Li *et al.* 2019). For example, gene expression levels measured in tissue samples by
59 direct RNA sequencing (RNA-seq) is now readily available to animal breeders (Ozsolak and
60 Milos 2011). To incorporate these new sources of data into genomic prediction models
61 requires new strategies for integration with the already widely used genome-wide marker data.
62 Although most of the literature focusing on the inclusion of gene-expression data into genomic

63 models to improve predictive performance aimed at predicting phenotypes (Takagi *et al.* 2014;
64 Guo *et al.* 2016; Schrag *et al.* 2018; Azodi *et al.* 2019; Li *et al.* 2019; Morgante *et al.* 2020),
65 fitting gene transcript levels as an additional layer of information into genomic models could
66 indirectly improve the prediction of breeding values. Christensen *et al.* (2021) presented a two-
67 step method to incorporate such intermediate omics into genomic evaluations considering
68 complete and incomplete omics-data scenarios. Results were validated using simulated data
69 and suggested superiority of the single-step method including both the intermediate omics and
70 genomics data, over the traditional genomic best linear unbiased prediction (GBLUP) using
71 only genomics data. Similar results were observed by Michel *et al.* (2021) when investigating
72 the integration of gene expression into genomic prediction for disease resistance in wheat by
73 using a hybrid relationship matrix for merging both layers of omics data. A pending issue that
74 remains, is the adequate handling of associations between layers of data that may lead to
75 inflated relative contributions of individual layers when ignored (Holm *et al.* 2010; Christensen
76 *et al.* 2021). Wade *et al.* (2021) have suggested that the benefits of multi-omics integration
77 models over single-omic models are achieved once redundancy of predictors is decreased.
78 Therefore, multi-omics models should either automatically or through adequate
79 parametrization be able to identify and manage information redundancy across multiple omics-
80 layers.

81 In the present study we used data from the Diversity Outbred (DO) mouse population
82 (Churchill *et al.* 2012; Svenson *et al.* 2012) to evaluate the utility of gene expression in addition
83 to genome-wide genetic markers for genomic prediction using different modeling strategies.
84 To this end, the objectives of this study were to: (1) assess the proportions of phenotypic
85 variance explained by genetic markers and gene transcripts in complex traits recorded in at
86 least two time points; (2) evaluate the predictive accuracy for phenotypes using transcripts
87 and/or marker information for the traits investigated using linear models and the gradient
88 boosting algorithm; and (3) evaluate how the inclusion of transcripts affects estimation of
89 genomic breeding values (GEBV) from BLUP models. The linear models proposed vary in

90 number of components, how interactions were modeled, and conditioning of one component
91 on another. The gradient boosting machine algorithm was chosen for its ability to automatically
92 control redundancy and implicitly account for non-linear effects in prediction, while the BLUP
93 models tested comprise parametric approaches to incorporate genomics and transcriptomics,
94 considering or ignoring the interactions between them.

95

96 MATERIAL AND METHODS

97 **Data**

98 *Phenotypes*

99 Data used for this study were obtained from The Jackson Laboratory (Bar Harbor, ME)
100 and comprise a subset of the dataset used in Perez *et al.* (2022). The 478 DO mice originated
101 from 4 non-overlapping generations (4, 5, 7 and 11) with males and females represented
102 equally. The total number of animals per generation was 47, 47, 192 and 192 for generations
103 4, 5, 7 and 11, respectively, with slight variation in the numbers of missing records across
104 traits (Table 1). The mice were maintained on either standard high fiber (chow, n=239) or high
105 fat diet (n=239) from weaning until 23 weeks of age. The proportion of males and females
106 within each diet category was close to 50-50 for all generations, as well as within each litter-
107 generation combination (two litters per generation). This population is maintained under a
108 systematic mating scheme, designed to limit population structure and relatedness. On
109 average, the animals were related to each other at a level equivalent to first cousins, which is
110 by design (Svenson *et al.* 2012). More elaborate descriptions of population structure,
111 husbandry and phenotyping methods can be found in Svenson *et al.* (2012) and Tyler *et al.*
112 (2021).

113 Table 1 gives for each trait a brief description, the numbers of observations and the
114 estimated heritability. We considered six traits based on range of heritability and presumed
115 genetic architectures. The chosen traits were measured at two or three times during the

116 animal's life, resulting in 13 distinct traits in total. The analyzed traits were bone mineral density
117 at 12 (BMD12) and 21 (BMD21) weeks, body weight at 10, 15 and 20 weeks (BW10, BW15
118 and BW20); circulating cholesterol at 8 (CHOL8) and 19 (CHOL19) weeks, adjusted body fat
119 percentage at 12 (FATP12) and 21 (FATP21), circulating glucose at 8 (GLUC8) and 19
120 (GLUC19) weeks, circulating triglycerides at 8 (TRGL8) and 19 weeks (TRGL19). These traits
121 can be categorized into measurements of body composition (bone mineral density, body
122 weights and fat percentage) and clinical plasma chemistries (circulating glucose and
123 triglycerides). Phenotypic records were pre-corrected for fixed effects of diet, generation, litter,
124 and sex (Perez *et al.* 2022). Therefore, the pre-corrected phenotypes (y^*) analyzed here
125 comprise the sum of the additive genetic effect and residual terms.

126

127 **TABLE 1**

128

129 *Genotypes*

130 The genotype data used for the animals in this study, were obtained from their derived
131 founder haplotypes (for details: see Perez *et al.* 2022). The complete genotype file used for
132 the analyses included 64,000 markers on an evenly spaced grid, and the average distance
133 between markers was 0.0238 cM. The full genotype dataset was cleaned based on the
134 following criteria: variants with minor allele frequency < 0.05, call rates < 0.90 and linear
135 correlation between subsequent SNPs > 0.80 were removed. After quality control, a total of
136 50,122 SNP markers were available for the mice with phenotypic, genotypic and
137 transcriptomic records.

138

139 *Transcript levels*

140 Transcriptome-wide expression levels were measured from whole livers as previously
141 described (Munger *et al.* 2014; Chick *et al.* 2016) for 478 animals at 26 weeks of age. The

142 RNA sample was sequenced using single-end RNA-Seq (Munger *et al.* 2014) and aligned
143 transcripts to strain-specific genomes from the DO founders (Chick *et al.* 2016). Read counts
144 were estimated using an expectation maximization algorithm (EMASE,
145 <https://github.com/churchill-lab/emase>). Read counts were previously corrected for the effects
146 of sex, diet, and batch by normalizing in each sample using upper quantile normalization and
147 applying a rank Z transformation across samples. After quality control, quantification of
148 transcripts was available for 11,770 genes (Tyler *et al.* 2017).

149

150 **Statistical models**

151 Below we introduce five best linear unbiased prediction (BLUP) models and three
152 gradient boosting machine (GBM) models with their acronyms and key features summarized
153 in Table 2.

154 **Best linear unbiased prediction**

155 **GBLUP**

156 The statistical model of GBLUP is:

157
$$\mathbf{y}^* = \mathbf{1}\mu + \mathbf{g} + \mathbf{e},$$

158 where \mathbf{y}^* is the vector of pre-corrected phenotypes, $\mathbf{1}$ is a vector of ones, μ is the
159 intercept, \mathbf{g} is the vector of random additive genetic values, where $\mathbf{g} \sim N(\mathbf{0}, \mathbf{G}\sigma_g^2)$, \mathbf{G} is the
160 additive genomic relationship matrix between genotyped individuals, and σ_g^2 is the additive
161 genomic variance. The matrix \mathbf{G} is constructed following the second method described by
162 VanRaden (2008) as $\frac{\mathbf{Z}\mathbf{Z}'}{m}$ where \mathbf{Z} is the matrix of centered and standardized genotypes for all
163 individuals and m is the number of markers. Finally, \mathbf{e} is the vector of random residual effects
164 where $\mathbf{e} \sim N(\mathbf{0}, \mathbf{I}\sigma_e^2)$ with σ_e^2 being the residual variance, and \mathbf{I} is an identity matrix.

165

166 **TBLUP**

167 To evaluate the performance of transcriptomic data for predicting complex traits, we
168 used a Transcriptomic Best Linear Unbiased Predictor (TBLUP) model. This model is similar
169 to GBLUP, but using a transcriptomic relationship matrix, which evaluates the similarity among
170 animals based on gene expression levels (Guo *et al.* 2016).

171 The statistical model of TBLUP is:

172
$$\mathbf{y}^* = \mathbf{1}\mu + \mathbf{t} + \mathbf{e},$$

173 where \mathbf{y}^* , $\mathbf{1}$ and μ are defined as above, \mathbf{t} is the vector of random transcript level effects,
174 where $\mathbf{t} \sim N(\mathbf{0}, \mathbf{T}\sigma_t^2)$ and \mathbf{T} is the transcriptomic relationship matrix built according to the
175 formula $\frac{\mathbf{W}\mathbf{W}'}{k}$ where \mathbf{W} is the matrix of centered and standardized expression levels for all
176 animals and k is the number of genes, and σ_t^2 is the variance explained by gene transcripts.

177

178 **GTBLUP and GTIBLUP**

179 The GTBLUP model fitted the \mathbf{g} and \mathbf{t} as independent random effects, each with their
180 own variance component (Guo *et al.* 2016; Li *et al.* 2019). The model is $\mathbf{y}^* = \mathbf{1}\mu + \mathbf{g} + \mathbf{t} + \mathbf{e}$,
181 where all the parameters are as defined above.

182 The GTIBLUP model fitted \mathbf{g} , \mathbf{t} , and the interaction between \mathbf{g} and \mathbf{t} with an additional
183 variance component (Morgante *et al.* 2020). This model is $\mathbf{y}^* = \mathbf{1}\mu + \mathbf{g} + \mathbf{t} + \mathbf{gt} + \mathbf{e}$,
184 where \mathbf{y}^* , $\mathbf{1}\mu$, \mathbf{g} , \mathbf{t} and \mathbf{e} are as defined above, and \mathbf{gt} is the vector of interaction (between
185 genomic and transcriptomic) effects, where $\mathbf{gt} \sim N(\mathbf{0}, \mathbf{G}\#\mathbf{T}\sigma_{gt}^2)$ and $\#$ is the Hadamard
186 product.

187

188

189

190 **GTCBLUP**

191 The GTCBLUP model was similar to GTBLUP in that the **g** and **t** that were fitted as
192 independent random effects, each with their own variance component. However, for this model
193 the transcript levels were conditioned on SNP genotypes, yielding a matrix **W_c** computed as:
194
$$\mathbf{W}_c = (\mathbf{I} - \mathbf{Z}(\mathbf{Z}'\mathbf{Z} + \mathbf{I}\lambda)^{-1}\mathbf{Z}')$$

$$\mathbf{W}$$
, where $\mathbf{Z}(\mathbf{Z}'\mathbf{Z} + \mathbf{I}\lambda)^{-1}\mathbf{Z}'$ is the so-called “smoother matrix”
195 (Hastie *et al.* 2009), **Z** is the matrix of centered and standardized genotypes as before, **I** is an
196 identity matrix, and $\lambda = \frac{m * \sigma_e^2}{\sigma_g^2}$, σ_e^2 is the residual variance, and σ_g^2 is the additive genomic
197 variance, both variances estimated with the GBLUP model (including only **g**). Using the
198 smoother matrix, i.e. including $\mathbf{I}\lambda$ rather than using $\mathbf{I} - \mathbf{Z}(\mathbf{Z}'\mathbf{Z})^{-1}\mathbf{Z}'$, reflects that the effects
199 associated with the SNPs are estimated as random rather than fixed effects. The aim of this
200 model is to remove any variance from transcripts that is correlated to variance in genotypes,
201 such that any phenotypic variance both associated with variance in genotypes and transcripts
202 automatically will be associated with the genotypes only. The model is $\mathbf{y}^* = \mathbf{1}\mu + \mathbf{g} + \mathbf{t}_c + \mathbf{e}$,
203 where $\mathbf{t}_c \sim N(\mathbf{0}, \mathbf{T}_c \sigma_t^2)$ and \mathbf{T}_c is computed as $\frac{\mathbf{W}_c \mathbf{W}_c'}{k}$, and all other parameters are as defined
204 above.

205

206 **Gradient boosting machine models**

207 Gradient boosting machine (GBM) is an ensemble learning technique that applies an
208 iterative process of assembling “weak learners” into a stronger learner, being largely used for
209 both classification and regression problems (Friedman 2001). In the scope of this
210 investigation, the GBM algorithm represents a non-parametric approach capable of implicitly
211 fitting not only the additive effects of SNP and gene transcripts, but also the within- and
212 between-omics layers interactions. The GBM is also capable of performing automatic feature
213 selection, prioritization of important variables and discarding variables containing irrelevant or
214 redundant information. A detailed description of the gradient boosting machine algorithm and

215 its application in genomic prediction can be found in Friedman (2002), González-Recio *et al.*
216 (2010; 2013) and Perez *et al.*, (2022).

217 To obtain the best possible results from the GBM algorithm, a grid search approach
218 was used to determine the combination of hyperparameters that minimized the mean squared
219 error of prediction within the inner training set for each trait. Details of the hyperparameter
220 search method used are found in Perez *et al.* (2022). We implemented the GBM model using
221 the “gbm” R package (Ridgeway 2020).

222 We tested three different GBM models. The first model considered only SNP
223 genotypes as predictors (GGBM), the second model considered only (standardized) gene
224 transcript levels as predictors (TGBM) and a third model that considered both genetic markers
225 and transcript levels together as predictors (GTGBM). Our objective was to investigate if GBM
226 models could capture within and between omics layers associations, while also reducing within
227 and between omics layers redundancy by performing automatic variable selection. It is
228 important to note here that although here we used “G” and “T” letters to refer to genomics and
229 transcriptomics data in the GBM model’s acronyms, predictors were fit directly in the model
230 and not as relationship matrices

231

232 **TABLE 2**

233

234 ***Variance explained by genetic markers, transcript levels and combinations of both***

235 To understand how much of the phenotypic variance can be explained by using SNP
236 genotypes, gene transcript levels and the combinations of both sources of information, we
237 estimated variance components using the GBLUP, TBLUP, GTBLUP, GTIBLUP and
238 GTCBLUP models. Estimates of variance components along with the residual variance (σ_e^2)
239 were obtained from a Bayesian approach analysis, using the BGLR R package (Pérez and de

240 los Campos 2014). For all models, the Gibbs sampler was run for 60,000 iterations, with a
241 20,000 burn-in period and a thinning interval of 10 iterations. Consequently, inference was
242 based on 4,000 posterior samples.

243 For the GTIBLUP model, we calculated the portion of variance explained by SNP
244 genotypes ($h^2 = \frac{\sigma_g^2}{\sigma_g^2 + \sigma_t^2 + \sigma_{gt}^2 + \sigma_e^2}$), gene transcripts ($t^2 = \frac{\sigma_t^2}{\sigma_g^2 + \sigma_t^2 + \sigma_{gt}^2 + \sigma_e^2}$) and from the interaction
245 between effects from genetic markers and gene transcripts ($gt^2 = \frac{\sigma_{gt}^2}{\sigma_g^2 + \sigma_t^2 + \sigma_{gt}^2 + \sigma_e^2}$).
246 Consequently, the sum of h^2 , t^2 and gt^2 represent the portion of phenotypic variance
247 explained by two layers of omics data and by the between-omics-layer interactions. The
248 parameters h^2 , t^2 and gt^2 for the other models were calculated similarly but omitted any
249 variance components associated with effects not included in the model.

250 *Model Performance*

251 Performance of predictions from the models was measured by the accuracy, computed
252 as the Pearson correlation ($r_{y^*,\hat{y}}$), and the relative root-mean squared error of prediction
253 (RRMSE) between predictions (\hat{y}) and pre-corrected phenotypes (y^*): $RRMSE =$
254 $\sqrt{\frac{1}{n} \sum_{i=1}^n (y^* - \hat{y})^2 / \sigma_p}$, where σ_p is the phenotypic standard deviation. In all analyses, we
255 used a forward prediction validation scheme in which animals from older generations (4, 5, 7)
256 were used as the reference and animals from the younger generation (11) as the validation
257 subset. The standard error (SE) around the $r_{y^*,\hat{y}}$ estimates were obtained by calculating the
258 standard deviations from 10,000 bootstrap samples (Davison and Hinkley 1997). The
259 bootstrapping procedure was implemented using the “boot” R package (Canty and Ripley
260 2021). We have also assessed prediction bias by obtaining the regression coefficient from the
261 linear regression of corrected phenotypes on model predictions. For these results, values
262 above 1 indicate deflation, while values below 1 indicate inflation of predicted values.

263 To assess the proportion of variance explained by the models tested, we have
264 calculated the coefficient of determination (R^2) from the regression of corrected phenotypes
265 on model predictions for all traits. For the GBM models we have used results from the model
266 using the previously obtained best hyperparameter set from the standard grid-search
267 procedure to assess the model R^2 for prediction within the reference set.

268 For the BLUP models proposed to integrate SNP genotypes and gene transcripts
269 (GTBLUP, GTIBLUP and GTCBLUP), in addition to $r_{y^*,\hat{y}}$ we have also calculated the
270 correlations between the solutions for each random effect included in the model (g , t , t_c or
271 gt) and \hat{y} , as well as pairwise comparisons between all components in the model. Here, we
272 also focus on solutions from the additive genetic component from these models to assess if
273 the prediction of genomic breeding values (GEBV) can be improved by using models capable
274 of integrating SNP genotypes and gene transcripts for genomic prediction.

275

276 **Data Availability**

277 All data associated with this manuscript, and the code developed and used to perform
278 analyzes described in this manuscript, can be obtained at
279 <https://doi.org/10.6084/m9.figshare.15081636.v1>. All software used is publicly available.

280

281 **RESULTS**

282 ***Variance components estimation percentage of variance explained within the*** ***reference set***

284 Genomic heritabilities (h^2) obtained with GBLUP ranged from 0.08 to 0.44,
285 representing a wide range of magnitudes across traits (Figure 1 and Figure 2). When only
286 fitting transcript levels as predictors (TBLUP), the percentage of variance explained (t^2)
287 ranged from 0.22 to 0.75 and in general it was higher than h^2 when comparing within the same
288 trait. The exceptions to that were observed for BMD12 ($h^2 = 0.39$ and $t^2 = 0.35$) and GLUC8
289 ($h^2 = 0.30$ and $t^2 = 0.22$). When comparing the same trait measured at different time points,

290 t^2 from TBLUP was higher for phenotypes collected closer to the 26 weeks of age (i.e. the
291 age at mRNA data sampling).

292 In terms of the total phenotypic variance explained, GTBLUP and GTIBLUP showed
293 similar results (Figure 1 and Figure 2). For body weights (BW10, BW15, BW20) and fat
294 percentage (FATP12 and FATP21) traits, the variance explained by genetic markers (in
295 GTBLUP and GTIBLUP) was drastically lower when compared to GBLUP for the same traits.
296 For the remaining traits the decrease in genetic variance captured by markers was much
297 lower. For the interaction component in GTIBLUP (gt^2), results observed varied according to
298 the trait analysed but in general, it was low compared to h^2 and t^2 . The only exception to that
299 was observed for TRGL8, in which gt^2 was higher than h^2 and t^2 . For CHOL8, GLUC19 and
300 TRGL19, gt^2 was either similar to h^2 or t^2 .

301 For GTCBLUP, differently from GTBLUP and GTIBLUP, the additive genetic variance
302 captured was always in line with results from GBLUP. On the other hand, the variance
303 explained by transcripts (t^2) from GTCBLUP was always lower than observed by other models
304 including transcripts as predictors (TBLUP, GTBLUP and GTIBLUP).

305

306 **FIGURE1**

307 **FIGURE 2**

308

309 The variance explained (represented by the R^2 parameter) within the reference data
310 by parametric models was in general lower than by the non-parametric counterparts (Table
311 3). Independent of being a parametric or non-parametric model, the use of gene transcripts
312 (TBLUP and TGBM) as predictors explained in most cases more of the variance than using
313 exclusively SNP genotypes (GBLUP and GGBM). For GTBLUP, GTIBLUP and GTGBM, the
314 variance explained was at least similar to observed for TBLUP and TGBM, but generally

315 higher. For GTCBLUP, variance explained by the model was slightly to moderately higher than
316 observed for GBLUP model, but always smaller than observed for GTBLUP, GTIBLUP and
317 GTGBM. The average R^2 when considering only traits recorded earlier (suffixes 8, 10 or 12)
318 and later (suffixes 19, 20 or 21) moments were 76% and 83%, respectively, when using
319 TBLUP, being the largest difference observed across models when considering these two
320 groups of traits.

321

322 **TABLE 3**

323 ***Prediction performance – Phenotype prediction***

324 In Table 4 accuracies are shown for predicted phenotypes for BLUP and GBM models
325 using either SNP genotypes, transcript levels or both as predictors. Here we considered
326 GBLUP to be the reference method. It showed prediction accuracies ranging from 0.01 to
327 0.29, these were highly positively correlated to the portion of variance explained by SNP
328 genotypes by the same model, except for CHOL19. When comparing predictive performance
329 between GBLUP and GGBM models, GBLUP yielded highest prediction accuracies for 7 traits,
330 while GGBM had best predictive performance for 6 traits out of 13.

331 For models that include only gene transcripts (TBLUP and TGBM), the TBLUP
332 approach showed predictive accuracies ranging from 0.03 to 0.61, having the best
333 performance for only 4 out of 13 traits. The TGBM model was able to overcome TBLUP for 7
334 traits, with prediction accuracies ranging from 0.04 to 0.58. For BMD21 and BW15, predictive
335 accuracy was identical between TBLUP and TGBM. The differences between accuracies from
336 TBLUP and TGBM was higher than between GBLUP and GGBM.

337 For models that combined SNP genotypes and gene transcripts levels (GTBLUP,
338 GTCBLUP, GTIBLUP and GTGBM), GTBLUP had the highest predictive accuracy for 5 traits
339 out of 13. The second-best model overall was GTGBM, with the highest predictive accuracy
340 for 4 traits. For every trait that GTIBLUP had the highest prediction accuracy, it was identical

341 to the result for GTBLUP, while the GTCBLUP never had the highest predictive accuracy
342 (Table 4).

343 The prediction error (RRMSE) and bias (β) for model's predictions are presented in
344 Supplementary Tables S1 and S2, respectively. Considering single-omics models, on average
345 BLUP models (GBLUP and TBLUP) yielded less biased predictions than GBM models (GGBM
346 and TGBM). For models integrating SNP genotypes and gene transcripts, GTBLUP and
347 GTIBLUP showed similar bias across traits, while GTGBM had on average less bias than the
348 BLUP models. For the GTCBLUP model, predictions were inflated ($\beta < 1$) for all traits but
349 BMD21. In terms of prediction error, differences between models were smaller than observed
350 for bias (Supplementary Table S2) or predictive accuracies (Table 4). The lowest RRMSE
351 values were observed for FATP21, while the highest were observed for GLUC19. The RRMSE
352 values for all traits analyzed were all around 1, indicating the average prediction errors were
353 close to one phenotypic standard deviation.

354

355 **TABLE 4**

356

357 ***Predictive ability for GEBV and other model components, and the correlation between***
358 ***them in BLUP models***

359 In Table 5 the Pearson's coefficient correlation between model components solutions
360 (\hat{g} , \hat{t} , \hat{t}_c and \hat{g}_t) for the different BLUP models and corrected phenotypes (y^*) are shown.
361 Overall, results for GTBLUP and GTIBLUP were similar across traits. These two models had
362 the most accurate GEBV ($\rho_{\hat{g}, y^*}$) exclusively for GLUC8, while for BMD12 results from these
363 models were matched by GTCBLUP. For GLUC19, all four parametric multi-omics models
364 yielded the same accuracy for GEBV, which was the lowest (0.01) across traits. In 8 out of 13
365 traits the GEBV estimated using GTCBLUP model was the most accurate across all models.
366 The correlation between \hat{t} and y^* ($\rho_{\hat{t}, y^*}$) was also similar between GTBLUP and GTIBLUP,
367 being always higher for these two models than observed for GTCBLUP. For

368 GTCBLUP exclusively, $\rho_{\hat{t}_y^*}$ was low and negative for CHOL19 (-0.08), GLUC19 (-
369 0.05) and TRGL8 (-0.07). For most traits, although a slight increase in the total
370 variance explained was observed within the reference dataset (Figures 1 and 2) when
371 comparing GTBLUP and GTIBLUP, there was not a proportional increase in $\rho_{\hat{g}_y^*}$ in
372 the validation (Table 5). For GTCBLUP on the other hand, for all traits there was an
373 increase in the variance explained by SNP genotypes (g^2 in Figure 1 and Figure 2)
374 when compared to GTBLUP and GTIBLUP, and the same pattern was observed for
375 $\rho_{\hat{g}_y^*}$. Results for $\rho_{\hat{g}_t}$ varied from +0.14 to +0.29 for GTBLUP and from +0.13 to +0.29
376 for GTIBLUP. For GTCBLUP, values for $\rho_{\hat{g}_t^c}$ were all negative and close to zero,
377 ranging from -0.13 to -0.03 (Table 5). The values for $\rho_{\hat{g}_t^g}$, only calculated for GTIBLUP,
378 were close to zero for most traits with an exception for CHOL8 and CHOL19, for which
379 $\rho_{\hat{g}_t^g}$ was 0.18. A similar pattern was observed for $\rho_{\hat{t}_g^t}$, for which values varied from -
380 0.12 to +0.06, with the largest differences from $\rho_{\hat{g}_t^g}$ observed for CHOL8 and CHOL19.

381

382

TABLE 5

383

384 DISCUSSION

385 Here, we investigated parametric and non-parametric approaches to leverage
386 transcriptomic data for the prediction of complex phenotypes. To accomplish that, we used
387 478 animals from the DO Mouse population (Svenson *et al.* 2012), for which information on
388 phenotypes (Churchill *et al.* 2012) for a wide range of quantitative traits, SNP genotypes and
389 gene transcript levels from liver tissue (Tyler *et al.* 2017) were available on the same animals.
390 We used the genomic (GBLUP) and transcriptomic (TBLUP) best linear unbiased prediction
391 models to evaluate the value of these omics data to predict phenotypes. In addition, we
392 evaluated models to integrate genome and transcriptome data by modelling both layers

393 independently (GTBLUP) or including an interaction component between the genome and
394 transcriptome (GTIBLUP). Finally, we proposed the GTCBLUP model that removes the
395 between-omics-layer information redundancy. The gradient boosting machine (GBM)
396 algorithm was investigated as a non-parametric approach potentially able to perform variable
397 selection and capture non-linear effects by fitting either SNP genotypes (GGBM), gene
398 transcript levels (TGBM) or to integrate both layers implicitly modeling interactions within and
399 between omics layers (GTGBM).

400 Using data from six distinct traits measured at two or three time points (resulting in 13
401 traits in total), we first assessed the proportion of phenotypic variance explained by each
402 variance component in the parametric models (Figure 1 and Figure 2). The variance explained
403 by SNP genotypes and gene transcript levels (and their interaction) varied by trait, time of
404 measurement and the model used. When using transcripts as predictors, two main patterns
405 were observed. For 5 out 13 traits (Figure 1), the TBLUP model explained much more of the
406 phenotypic variance than GBLUP. For the other 8 out of 13 traits (Figure 2), TBLUP explained
407 less variance than GBLUP. The observation that the portion of variance explained by gene
408 transcripts is strongly trait-specific is in line with results observed when assessing the
409 proportion of variance from gene transcripts for complex traits in *Drosophila* (Morgante *et al.*
410 2020). Ehsani *et al.* (2012) have analyzed data from an F2 mice population using models
411 integrating genotype markers and liver transcriptomics data. The authors reported that
412 transcripts explained 79%, while genotypes explained 36% of the phenotypic variance for body
413 weight at 8 weeks of age. It is important to emphasize that in Ehsani *et al.*, (2012), RNA
414 samples were measured at the same time point as phenotypes were collected. Other authors
415 have observed that the genetic markers always explained a bigger portion of variance than
416 transcripts in maize (Guo *et al.* 2016; Azodi *et al.* 2019) and *Drosophila* (Li *et al.* 2019).

417 There are several possible reasons for the conflicting results found in literature when
418 assessing the value of transcripts to explain variation in complex phenotypes. Differently from
419 genotypes, transcripts are affected by many factors such as the tissue from where samples

420 are collected, the moment in life of sampling and the environmental conditions that the animal
421 was exposed to. These variables most likely impact the variance explained (and concomitantly
422 prediction performance) by transcripts. In Azodi *et al.* (2019) for example, transcripts were
423 quantified from whole seedlings while phenotypes were recorded at a much older age, which
424 could explain the limited predictive ability of transcriptomics data. In the present study
425 transcripts were measured when the mice were 26 weeks of age, while all phenotypes were
426 recorded at younger ages (from 8 to 21 weeks of age). In our results, phenotypes recorded
427 closer to 26 weeks of age had a larger proportion of phenotypic variance explained by
428 transcripts than measurements made earlier in the animal's life for the same phenotype
429 (Figure 1 and Figure 2). For BW and FATP the transcripts explained a larger proportion of
430 phenotypic variance at all time points. For BMD, CHOL, GLUC and TRGL this was the case
431 when there was 4 (BMD) to 6 weeks (CHOL, GLUC and TRGL) in-between measuring
432 phenotypes and transcripts, while genomics explained more phenotypic variance when this
433 time frame increased to 14 (BMD) or 18 weeks (CHOL, GLUC and TRGL) in-between. It is
434 important to emphasize here that although this outcome may have been expected beforehand,
435 to our knowledge it is the first time that this link between amount of variance explained by
436 transcript versus the time difference between measuring transcripts and phenotypes has been
437 shown empirically. One other aspect that must be considered here is that the gene expression
438 from whole maize seedlings (Azodi *et al.* 2019) is probably much less related to traits collected
439 later in life than the gene expression from liver tissue available for the DO mouse dataset. It
440 is widely known that the liver is strongly linked to many metabolic pathways (Ponsuksili *et al.*
441 2019), and therefore likely also especially to the BW and FATP traits used here, while the
442 variation contained in a sample collected from whole seedlings do not reflect a specific tissue
443 but a pool of all tissues in this organism.

444 When fitting both SNP genotypes and gene transcripts as predictors the portion of
445 variance explained by SNP genotypes varied drastically from the GBLUP model. For all BW
446 and FATP traits, the proportion of variance explained by genotypes using GTBLUP and

447 GTIBLUP was much lower than for GBLUP. Ehsani *et al.* (2012) and Takagi *et al.* (2014)
448 observed a reduction in captured genetic variance by SNP genotypes of around 50% when
449 fitting genotypes together with transcripts compared to models using fitting only genotypes as
450 predictors for complex traits in other mice populations. This seems to confirm the hypothesis
451 that there is redundant information between the genome and transcriptome layers (Wade *et*
452 *al.* 2021), as also shown to be the case in *Drosophila* (Morgante *et al.* 2020). In our experience,
453 it seems that the closer the phenotype analyzed is to the moment of RNA sampling, the higher
454 the decrease in genetic variance captured by SNP genotypes in GTBLUP and GTIBLUP. This
455 was observed for almost all traits we analyzed in different magnitudes. Takagi *et al.* (2014)
456 analyzed circulating cholesterol at 10 weeks of age in mice and reported a large decrease in
457 the genetic variance captured from SNP genotypes from models including only SNP
458 genotypes ($g^2= 46\%$) and together with liver transcripts ($g^2= 19\%$) also measured at 10 weeks
459 of age. In the present study, we observed only a slight decrease in genetic variance estimated
460 when comparing GTBLUP ($g^2= 28\%$) and GBLUP ($g^2= 38\%$) for CHOL8. This seems to
461 confirm that for the same phenotype, measurements made closer to the RNA sampling are
462 prone to exhibit this pattern in a higher magnitude than measurements. This was further
463 substantiated by the results observed for GTCBLUP. By conditioning the transcripts on the
464 genotypes, the portion of variance explained by SNP genotypes was similar to the GBLUP
465 model, while the variance explained by gene transcripts was much lower than estimated with
466 TBLUP, GTBLUP and GTIBLUP.

467 The formal variance partitioning achieved with the BLUP models cannot be achieved
468 with the non-parametric GBM models. To compare the performance of GBM and BLUP in
469 terms of explained variance we investigated the model R^2 within the reference set. For the
470 GBM models it was almost always higher than for the BLUP models (Table 3). From our
471 results, this pattern is recognizable for almost all traits analyzed, in which the GBM algorithm
472 is able to capture a higher portion of variance than the parametric counterpart within the
473 reference dataset (Table 3) but fails to outperform these models when predicting in the

474 validation set (Table 4). The only exception to that is observed for GLUC19, for which in
475 addition to the much larger portion of variance explained within the reference set, the GBM
476 algorithm also outperformed BLUP models by a large margin for prediction purposes. The
477 presence of noise in the data, limited size of the training set and the underlying complexity of
478 the event being modelled are often cited as common causes of overfitting in machine learning
479 models (Vabalas *et al.* 2019; Ying 2019). Here we used a training dataset of 286 animals and
480 the high number of predictors in the models, coupled with the unavoidable presence of
481 collinearity within and between omics layers may have caused GBM models to overfit. Takagi
482 *et al.* (2014) have also analyzed datasets of similar size from another heterogeneous mice
483 population using parametric models that integrated genomics and transcriptomics data,
484 reporting large portions of phenotypic variance captured within training sets that weren't
485 necessarily translated to high predictive accuracy in the validation set for circulating glucose
486 and cholesterol. The authors argue that the high number of model's parameters to be
487 estimated and the small number of animals with observations available could be the main
488 cause of this pattern. We have observed a big impact of hyperparameters on the in predictive
489 accuracies of the GBM models (results not shown). Having access to larger datasets could
490 help to elucidate the magnitude of this impact for the models analyzed here since it would
491 decrease the impact of hyperparameter definition in predictive performance, improving
492 strength of evidence for any differences found between GBM and other models tested. The
493 forward-prediction validation method adopted in the present study was previously described
494 in Perez *et al.* (2022) and mimics prediction in animal and plant breeding, where a predictive
495 model is trained based on data from individuals that have genomics (here also transcriptomics)
496 and phenotype data available, while prediction is intended for un-phenotyped younger
497 individuals. Here, training and validation generations were also 3 generations apart from each
498 other, which erodes strong relationships (e.g., parent-progeny) and therefore should not be
499 the cause of model overfitting suggested for the GBM models.

500 Prediction performance for phenotypes can be improved by combining genotypes and
501 transcripts, however our results suggested that the magnitude of improvement is dependent
502 on the trait analyzed (Table 4). In line with the observed differences in variance explained by
503 model components, TBLUP showed a better predictive ability than GBLUP for most traits
504 except CHOL19, GLUC8 and GLUC19. In contrast, Takagi *et al.* (2014) reported higher
505 predictive accuracies for circulating glucose and cholesterol when using liver transcripts as
506 predictors when compared to using genotypes in a different heterogeneous mice population
507 (Valdar *et al.* 2006). Two aspects may explain the differences observed between studies. First,
508 Takagi *et al.* (2014) performed a cross-validation scheme by randomly sampling individuals
509 as reference and validations sets while we performed a forward-validation scheme, in which
510 phenotype prediction for younger animals was based on estimates from older generations.
511 Even though animals are randomly sampled, the overall similarity between reference and
512 validation sets is higher in Takagi *et al.* (2014), which in general leads to higher magnitude of
513 predictive accuracy (Pszczola *et al.* 2012; Werner *et al.* 2020). It is important to emphasize
514 that although this is true when dealing exclusively with SNP genotypes, we cannot confirm
515 that the affirmative holds when dealing with transcripts as predictors. A second relevant aspect
516 is that in the present study phenotypes for CHOL and GLUC were collected at 8 and 19 weeks,
517 while RNA samples were taken at 26 weeks of age. As previously mentioned, in Takagi *et al.*
518 (2014) RNA samples and phenotypes were collected at the same age (10 weeks). In the
519 present study, phenotypes recorded at a closer time point to transcript profiling result in higher
520 predictive performance from transcripts (Table 4).

521 The TGBM model was able to overcome the TBLUP model for several traits, which
522 was not the case when comparing GBLUP and GGBM. This result may indicate that
523 interactions between transcripts were more easily captured or are more relevant than between
524 SNPs. When fitting only genotype markers, the model is limited by incomplete linkage
525 disequilibrium between the SNP and quantitative trait loci to perform an accurate detection of
526 possible interactions, while there is no such limiting factor when using gene transcripts. One

527 other hypothesis is that as transcripts are more strongly linked to phenotypes than genetic
528 markers, transcript-by-transcript interactions are also likely to affect the phenotype more
529 strongly than SNP-by-SNP interactions (Green *et al.* 2019), hence the former is expected to
530 have a clearer and more detectable signal. Morgante *et al.* (2020) have used the random
531 forest model, a non-parametric ensemble machine learning method like GBM, to predict
532 complex phenotypes in *Drosophila* using gene transcripts as predictors but did not observe a
533 superior predictive ability when compared to the TBLUP model. While TGBM consistently
534 outperformed TBLUP in our study, the GTGBM was only partly outperforming GTBLUP and
535 GTIBLUP. This could mean that the inclusion of SNP genotypes together with gene transcripts
536 as predictors in the GTGBM model may have impaired the ability of GBM to capture linear and
537 non-linear signals from within- and between-omics layers. The exact cause remains unclear,
538 but the size of dataset together with the substantial increase in number of predictors when
539 going from TGBM to GTGBM may be in the roots of it. It is likely that the GBM algorithm may
540 require more data to be able to accurately capture all patterns from the complex relationship
541 between omics layers underlying quantitative traits. If this is indeed the case, testing these
542 models using a larger dataset could help to confirm this hypothesis. In Azodi *et al.* (2019)
543 machine learning models integrating genomics and transcriptomics data were also not able to
544 outperform single-omics models in terms of predictive accuracy for three traits in maize using
545 a dataset of similarly limited size as in the present study.

546 The linear association for solutions from BLUP models' components predicted for
547 animals within the validation set were very similar between GTBLUP and GTIBLUP. For these
548 two models $\rho_{\hat{g}_y^*}$, $\rho_{\hat{t}_y^*}$ and $\rho_{\hat{g}_t}$ were almost identical across all traits (Table 5). Although the
549 inclusion of an interaction component in GTIBLUP captured between 9% and 26% of
550 phenotypic variance (represented by gt^2 in Figure 1 and Figure 2) within the reference set, it
551 did not seem to affect the relationship between other components. The low values observed
552 for $\rho_{\hat{g}_\text{gt}}$ and $\rho_{\hat{t}_\text{gt}}$ in GTIBLUP also seem to suggest that the interaction component is
553 capturing a portion of variance not directly shared with \hat{g} or \hat{t} components, and therefore it

554 does not affect the relationship between other components. The linear association between \hat{g}
555 and \hat{t} in GTBLUP and GTIBLUP models was always higher than the association between \hat{g}
556 and \hat{t}_c in GTCBLUP across all traits analyzed. Since in the GTCBLUP model the transcript
557 relationship matrix was conditioned on the variance of SNP genotypes (t_c), the linear
558 association between solutions for the two components was expected to closer to zero than
559 the observed in GTBLUP or GTIBLUP.

560 In this paper, we proposed the GTCBLUP model as an alternative to integrate genome
561 and transcriptome data for genomic prediction. There has been an increasing interest in the
562 use of intermediate omics data in animal and plant breeding (Guo *et al.* 2016; Yang *et al.*
563 2017; Azodi *et al.* 2019; Morgante *et al.* 2020; Christensen *et al.* 2021; Michel *et al.* 2021),
564 such as transcriptomics, metabolomics, or microbiome data. The inclusion of new layers of
565 omics data into genomic prediction models could arguably help in capturing additional portions
566 of variance not explained by genotype data, but at the same time, these layers most likely
567 contain overlapping information, increasing collinearity between predictors. Modelling the
568 relationship between G and T components could be an efficient way to realize the added value
569 of integrating such omics data into genomic prediction models (Wade *et al.* 2021), but this
570 could also be a challenge given the increase in number of parameters to be estimated. The
571 advantage of the GTCBLUP is that as pre-processing step it conditions the variance contained
572 in transcripts on the variance of genotypes to minimize the amount of redundant information
573 without having to increase model complexity. In general, the GTCBLUP model was able to
574 produce GEBV that were at least as accurate as or slightly more accurate than the GBLUP
575 model. The percentage of variance explained by SNP genotypes in GTCBLUP was similar to
576 that with the GBLUP model, while it was always lower when using GTBLUP and GTIBLUP
577 (Figure 1 and Figure 2). The observed reduction in additive genetic variance for GTBLUP and
578 GTIBLUP when compared to GBLUP indicates strong redundancy in information contained in
579 the genomic and transcriptomic layers. So, the conditioning of transcripts on SNP genotypes
580 in GTCBLUP allowed this model to perform a more accurate variance partitioning for the

581 additive genetic component, which consequently resulted in a more accurate estimation of
582 GEBV (Table 5). An interesting alternative way to consider the covariance between genomics
583 and transcriptomics layers, is by explicitly modelling it, as can be done using the CORE-
584 GREML method (Zhou *et al.* 2020), implemented in the MTG2 software (Lee and van der Werf
585 2016). We considered this method to evaluate its potential, as well as to try and assess the
586 magnitude of overlapping information between genotype and transcript data for the traits
587 analysed. Results (Supplementary Table S3) indicated correlations from -0.47 to +0.71, with
588 highest values observed for BW10, BW15, BW20, CHOL8 and CHOL19, FATP19 but the
589 correlation coefficient was never significantly different from 0. Coincidentally for most of these
590 traits GTCBLUP obtained the most accurate GEBV when compared to GBLUP, GTBLUP and
591 GTIBLUP. These trends seem to further support that, for specific traits, genomics and
592 transcriptomics layers contain largely overlapping information, and although removing this
593 redundancy does not result in more accurate phenotype prediction, it may contribute to obtain
594 more accurate GEBV and consequently could improve breeding decisions. The lack of
595 significance of the estimated correlations between genomics and transcriptomics data may be
596 due to the limited size of the data used here, while based on the results obtained in the present
597 study this does not provide a limitation for the GTCBLUP model.

598 One limitation of the GTCBLUP model is that it does not accommodate missing omics
599 information, so all reference individuals must have genomics and transcriptomics data
600 available. In the context of breeding programs, a situation in which all reference animals have
601 multiple omics data available is unlikely to happen due to high costs involved in the collecting
602 this kind of information. However, based on the observed decrease in costs of genotyping
603 which has enabled large-scale genotyping, we may expect similar developments for the costs
604 of transcriptomics and other intermediate phenotypes in the near future (Uzbas *et al.* 2019).
605 At the same time, there have been some recent model developments that enable including
606 other omics data in genomic prediction, when these other omics data are not available for all
607 animals (Christensen *et al.* 2021; Zhao *et al.* 2022).

608 **CONCLUSION**

609 We have assessed prediction models that incorporate genetic markers and
610 transcriptomics data in genomic prediction of complex phenotypes in mice. The proportion of
611 phenotypic variance explained by transcripts was almost always higher when traits were
612 measured closer to the time of measuring gene transcripts. While GBM models explained
613 more variance in the reference data, their predictive performance did not exceed the GBLUP
614 models. Models including SNP genotypes and gene transcripts did not consistently outperform
615 the best single-omics models to predict phenotypes. While TGBM model was able to
616 outperform TBLUP, this was not the case for GTGBM compared to GTBLUP and GTIBLUP.
617 The newly developed GTCBLUP model was able to force all phenotypic variance associated
618 with SNP genotypes into its additive genetic component, by conditioning gene transcripts on
619 SNP genotypes. GTCBLUP generally yielded considerably lower accuracies of phenotypic
620 predictions than the other models including SNP genotypes and gene transcripts, but it
621 showed the best accuracies for breeding values for most traits. We recommend using the
622 GTBLUP model for prediction of phenotypes, while the GTCBLUP should be preferred when
623 the aim is to estimate breeding values.

624

625 **FUNDING**

626 This study is part of the GENE-SWiCH project that received funding from the European
627 Union's Horizon 2020 research and innovation programme under grant agreement no.
628 817998. Gary Churchill acknowledges support by the National Institutes of Health (NIH) grant
629 R01 GM070683.

630

631 **CONFLICTS OF INTEREST**

632 The authors report no conflicts of interest related to the present manuscript. Bruno Perez and
633 Marco Bink are employees of Hendrix Genetics (Boxmeer, The Netherlands).

634

635 **REFERENCES**

636 Abdollahi-Arpanahi R, Gianola D, Peñagaricano F. 2020. Deep learning versus parametric
637 and ensemble methods for genomic prediction of complex phenotypes. *Genet Sel Evol.*
638 52:12.

639 Azodi CB, Bolger E, McCarren A, Roantree M, de los Campos G, Shiu S-H. 2019.
640 Benchmarking parametric and machine learning models for genomic prediction of
641 complex traits. *G3 (Bethesda)*. 9:3691-3702.

642 Carty A, Ripley B. 2021. *boot: Bootstrap R (S-Plus) Functions*. R package version 1.3-28.

643 Chawade A, Alexandersson E, Bengtsson T, Andreasson E, Levander F. 2016. Targeted
644 proteomics approach for precision plant breeding. *J Prot Res.* 15:638-646.

645 Chick JM, Munger SC, Simecek P, Huttlin EL, Choi K, Gatti DM, Raghupathy N, Svenson KL,
646 Churchill GA, Gygi SP. 2016. Defining the consequences of genetic variation on a
647 proteome-wide scale. *Nature*. 534:500-505.

648 Christensen OF, Börner V, Varona L, Legarra A. 2021. Genetic evaluation including
649 intermediate omics features. *Genetics*. 219:iyab130.

650 Churchill GA, Gatti DM, Munger SC, Svenson KL. 2012. The diversity outbred mouse
651 population. *Mamm Genome*. 23:713-718.

652 Davison AC, Hinkley DV. 1997. *Bootstrap methods and their application*. Cambridge
653 University Press, New York.

654 Ehsani A, Sørensen P, Pomp D, Allan M, Janss L. 2012. Inferring genetic architecture of
655 complex traits using Bayesian integrative analysis of genome and transcriptome data.
656 *BMC Genom.* 13:456.

657 Fernie AR, Schauer N. 2009. Metabolomics-assisted breeding: a viable option for crop
658 improvement? *Trends Genet.* 25:39-48.

659 Friedman JH. 2001. Greedy function approximation: a gradient boosting machine. *Ann Stat.*
660 29:1189-1232.

661 Friedman JH. 2002. Stochastic gradient boosting. *Comp Stat Data Anal.* 38:367-378.

662 Gianola D, de los Campos G, Hill WG, Manfredi E, Fernando R. 2009. Additive genetic
663 variability and the Bayesian alphabet. *Genetics*. 183:347-363.

664 González-Recio O, Jiménez-Montero JA, Alenda R. 2013. The gradient boosting algorithm
665 and random boosting for genome-assisted evaluation in large data sets. *J Dairy Sci*.
666 96:614-624.

667 González-Recio O, Weigel KA, Gianola D, Naya H, Rosa GJM. 2010. L-2-Boosting algorithm
668 applied to high-dimensional problems in genomic selection. *Genet Res*. 92:227-237.

669 Green RM, Leach CL, Diewert VM, Aponte JD, Schmidt EJ, Cheverud JM, Roseman CC,
670 Young NM, Marcucio RS, Hallgrímsson B. 2019. Nonlinear gene expression-phenotype
671 relationships contribute to variation and clefting in the A/WySn mouse. *Dev Dyn*.
672 248:1232-1242.

673 Guo Z, Magwire MM, Basten CJ, Xu Z, Wang D. 2016. Evaluation of the utility of gene
674 expression and metabolic information for genomic prediction in maize. *Theor Appl Genet*.
675 129:2413-2427.

676 Hastie T, Tibshirani R, Friedman J. 2009. *The Elements of Statistical Learning*. Springer, New
677 York.

678 Holm K, Melum E, Franke A, Karlsen TH. 2010. SNPexp - A web tool for calculating and
679 visualizing correlation between HapMap genotypes and gene expression levels. *BMC
680 Bioinformatics*. 11:600.

681 Lee SH, van der Werf JJJ. 2016. MTG2: an efficient algorithm for multivariate linear mixed
682 model analysis based on genomic information. *Bioinformatics*. 32:1420-1422.

683 Li Z, Gao N, Martini JWR, Simianer H. 2019. Integrating gene expression data into genomic
684 prediction. *Front Genet*. 10.

685 Meuwissen THE, Hayes BJ, Goddard ME. 2001. Prediction of total genetic value using
686 genome-wide dense marker maps. *Genetics*. 157:1819-1829.

687 Michel S, Wagner C, Nosenko T, Steiner B, Samad-Zamini M, Buerstmayr M, Mayer K,
688 Buerstmayr H. 2021. Merging genomics and transcriptomics for predicting Fusarium head
689 blight resistance in wheat. *Genes*. 12:114.

690 Morgante F, Huang W, Sørensen P, Maltecca C, Mackay TFC. 2020. Leveraging multiple
691 layers of data to predict drosophila complex traits. *G3 (Bethesda)*. 10:4599-4613.

692 Munger SC, Raghupathy N, Choi K, Simons AK, Gatti DM, Hinerfeld DA, Svenson KL, Keller
693 MP, Attie AD, Hibbs MA, *et al.* 2014. RNA-Seq alignment to individualized genomes
694 improves transcript abundance estimates in multiparent populations. *Genetics*. 198:59-
695 73.

696 Nayeri S, Sargolzaei M, Tulpan D. 2019. A review of traditional and machine learning
697 methods applied to animal breeding. *Ann Health Res Rev*. 20:31-46.

698 Ozsolak F, Milos PM. 2011. RNA sequencing: advances, challenges and opportunities. *Nat
699 Rev Gen*. 12:87-98.

700 Pérez-Enciso M, Zingaretti LM. 2019. A guide for using deep learning for complex trait
701 genomic prediction. *Genes*. 10:553.

702 Perez BC, Bink MCAM, Svenson KL, Churchill GA, Calus MPL. 2022. Prediction performance
703 of linear models and gradient boosting machine on complex phenotypes in outbred mice.
704 *G3 (Bethesda)*. 12:jkac039.

705 Pérez P, de los Campos G. 2014. Genome-wide regression and prediction with the BGLR
706 statistical package. *Genetics*. 198:483-495.

707 Ponsuksili S, Trakooljul N, Hadlich F, Methling K, Lalk M, Murani E, Wimmers K. 2019.
708 Genetic regulation of liver metabolites and transcripts linking to biochemical-clinical
709 parameters. *Front Genet*. 10:348.

710 Pook T, Freudenthal J, Korte A, Simianer H. 2020. Using local convolutional neural networks
711 for genomic prediction. *Front Genet*. 11:561497.

712 Pszczola M, Strabel T, Mulder HA, Calus MPL. 2012. Reliability of direct genomic values for
713 animals with different relationships within and to the reference population. *J Dairy Sci*.
714 95:389-400.

715 Ridgeway G. 2020. Generalized Boosted Models: A guide to the gbm package. <https://cran.r-project.org/web/packages/gbm/vignettes/gbm.pdf>. Accessed 5 September, 2021.

717 Schrag TA, Westhues M, Schipprack W, Seifert F, Thiemann A, Scholten S, Melchinger AE.

718 2018. Beyond genomic prediction: combining different types of *omics* data
719 can improve prediction of hybrid performance in maize. *Genetics*. 208:1373-1385.

720 Svenson KL, Gatti DM, Valdar W, Welsh CE, Cheng R, Chesler EJ, Palmer AA, McMillan L,
721 Churchill GA. 2012. High-resolution genetic mapping using the mouse diversity outbred
722 population. *Genetics*. 190:437-447.

723 Takagi Y, Matsuda H, Taniguchi Y, Iwaisaki H. 2014. Predicting the phenotypic values of
724 physiological traits using SNP genotype and gene expression data in mice. *PLOS ONE*.
725 9:e115532.

726 Tohge T, Fernie AR. 2015. Metabolomics-inspired insight into developmental, environmental
727 and genetic aspects of tomato fruit chemical composition and quality. *Plant Cell Physiol*.
728 56:1681-1696.

729 Tyler AL, El Kassaby B, Kolishovski G, Emerson J, Wells AE, Mahoney JM, Carter GW. 2021.
730 Effects of kinship correction on inflation of genetic interaction statistics in commonly used
731 mouse populations. *G3 (Bethesda)*. 11:jkab131.

732 Tyler AL, Ji B, Gatti DM, Munger SC, Churchill GA, Svenson KL, Carter GW. 2017. Epistatic
733 networks jointly influence phenotypes related to metabolic disease and gene expression
734 in diversity outbred mice. *Genetics*. 206:621-639.

735 Uzbas F, Opperer F, Sönmezler C, Shaposhnikov D, Sass S, Krendl C, Angerer P, Theis FJ,
736 Mueller NS, Drukker M. 2019. BART-Seq: cost-effective massively parallelized targeted
737 sequencing for genomics, transcriptomics, and single-cell analysis. *Genome Biol*. 20:155.

738 Vabalas A, Gowen E, Poliakoff E, Casson AJ. 2019. Machine learning algorithm validation
739 with a limited sample size. *PLOS ONE*. 14:e0224365.

740 Valdar W, Solberg LC, Gauguier D, Burnett S, Klenerman P, Cookson WO, Taylor MS,
741 Rawlins JNP, Mott R, Flint J. 2006. Genome-wide genetic association of complex traits in
742 heterogeneous stock mice. *Nat Genet*. 38:879-887.

743 VanRaden PM. 2008. Efficient methods to compute genomic predictions. *J Dairy Sci*.
744 91:4414-4423.

745 Wade AR, Duruflé H, Sanchez L, Segura V. 2021. eQTLs are key players in the integration
746 of genomic and transcriptomic data for phenotype prediction.
747 bioRxiv.2021.2009.2007.459279.

748 Werner CR, Gaynor RC, Gorjanc G, Hickey JM, Kox T, Abbadi A, Leckband G, Snowdon RJ,
749 Stahl A. 2020. How population structure impacts genomic selection accuracy in cross-
750 validation: implications for practical breeding. *Front Plant Sci.* 11:592977.

751 Whittaker JC, Thompson R, Denham MC. 2000. Marker-assisted selection using ridge
752 regression. *Genet Res.* 75:249-252.

753 Yang Y-I, Zhou R, Li K. 2017. Future livestock breeding: Precision breeding based on multi-
754 omics information and population personalization. *J Integr Agricult.* 16:2784-2791.

755 Ying X. 2019. An overview of overfitting and its solutions. *J Phys Conf Ser.* 1168:022022.

756 Zhao T, Zeng J, Cheng H. 2022. Extend mixed models to multi-layer neural networks for
757 genomic prediction including intermediate omics data.
758 *Genetics.* <https://doi.org/10.1093/genetics/iyac1034>.

759 Zhou X, Im HK, Lee SH. 2020. CORE GREML for estimating covariance between random
760 effects in linear mixed models for complex trait analyses. *Nat Comm.* 11:4208.

761 Zingaretti LM, Gezan SA, Ferrão LFV, Osorio LF, Monfort A, Muñoz PR, Whitaker VM, Pérez-
762 Enciso M. 2020. Exploring deep learning for complex trait genomic prediction in polyploid
763 outcrossing species. *Front Plant Sci.* 11:25.

764

765

766 **Table 1.** Number of available observations (N), the extended description of traits, age of the
767 animals at phenotype measurement, and estimated heritability.

Trait	N	Trait description	Age at measurement	Estimated heritability ¹
BMD12	471	Bone mineral density	12 weeks	0.39
BMD21	471	Bone mineral density	21 weeks	0.41
BW10	478	Body weight	10 weeks	0.42
BW15	478	Body weight	15 weeks	0.35
BW20	478	Body weight	20 weeks	0.37
CHOL8	474	Circulating cholesterol	8 weeks	0.38
CHOL19	474	Circulating cholesterol	19 weeks	0.45
FATP12	471	Body fat percentage	12 weeks	0.35
FATP21	471	Body fat percentage	21 weeks	0.32
GLUC8	425	Circulating glucose	8 weeks	0.31
GLUC19	425	Circulating glucose	19 weeks	0.22
TRGL8	473	Circulating triglycerides	8 weeks	0.36
TRGL19	473	Circulating triglycerides	19 weeks	0.31

768 ¹ Standard errors for the heritability ranged from 0.07 to 0.09

769

770 **Table 2.** Overview of models applied to SNP genotypes and/or individual levels of gene
771 transcripts.

Model acronym		Explanatory variables		
		SNP genotypes	Gene transcripts	Interaction modelled
GBLUP	GGBM	Yes	No	No
		Yes	No	Yes (Implicitly)
TBLUP	TGBM	No	Yes	No
		No	Yes	Yes (Implicitly)
GTBLUP		Yes	Yes	No
GTCBLUP		Yes	Yes	No
GTIBLUP		Yes	Yes	Yes (Explicitly)
	GTGBM	Yes	Yes	Yes (Implicitly)

772

773

774 **Table 3.** Model R² (x100) for the best linear unbiased prediction (GBLUP, GTBLUP,
775 GTCBLUP and GTIBLUP) and gradient boosting (GGBM, TGBM and GTGBM) approaches
776 within training data¹.

Trait ¹	Model ²							
	Only SNP		Only gene transcripts		SNP + gene transcripts			
	GBLUP	GGBM	TBLUP	TGBM	GTBLUP	GTIBLUP	GTCBLUP	GTGBM
BMD12	75	90	79	96	85	92	88	95
BMD21	84	85	88	93	87	96	92	98
BW10	78	92	93	96	91	95	90	97
BW15	75	87	91	94	93	96	94	96
BW20	80	87	92	93	95	97	95	97
CHOL8	84	85	69	97	80	93	87	98
CHOL19	82	83	85	95	88	96	92	98
FATP12	75	76	89	97	92	96	95	98
FATP21	80	82	93	97	95	97	94	98
GLUC8	77	85	66	95	81	93	87	97
GLUC19	62	80	67	96	75	90	84	98
TRGL8	65	81	62	92	80	96	88	97
TRGL19	71	86	70	96	78	95	84	98
Mean (all)	76	85	80	95	86	95	90	97
Mean (T1)	75	85	76	96	85	94	89	97
Mean (T2)	76	84	83	95	86	95	90	98

777 T1 = average R² of the column considering only traits recorded earlier in life (suffixes 8, 10 and 12).

778 T2 = average R² of the column considering only traits recorded later in life (suffixes 19, 20 and 21).

779 ¹For a description of the traits, see Table 1.

780 ²For a description of the models, see Table 2.

781 ³BW15 trait was ignored when calculating average performance considering exclusively T1 and T2.

782

783 **Table 4.** Accuracies of predicted pre-corrected phenotypes for the validation subset with the
784 proposed models. For each group of models, the result with the highest accuracy is
785 indicated in bold, identical results between two or more models are indicated in underline.

Trait ¹	Model ²							
	Only SNP		Only gene transcripts		SNP + gene transcripts			
	GBLUP	GGBM	TBLUP	TGBM	GTBLUP	GTIBLUP	GTCBLUP	GTGBM
BMD12	0.19	0.16	0.27	0.25	<u>0.27</u>	<u>0.27</u>	0.20	0.25
BMD21	0.29	0.28	<u>0.38</u>	<u>0.38</u>	0.42	0.40	0.29	0.38
BW10	0.18	0.20	0.48	0.42	<u>0.47</u>	<u>0.47</u>	0.19	0.42
BW15	0.15	0.12	<u>0.52</u>	<u>0.52</u>	<u>0.51</u>	<u>0.51</u>	0.22	0.49
BW20	0.18	0.16	0.61	0.58	<u>0.60</u>	<u>0.60</u>	0.30	0.54
CHOL8	0.14	0.17	0.14	0.15	0.18	0.17	0.16	0.16
CHOL19	0.25	0.20	0.19	0.16	0.26	0.23	0.22	0.23
FATP12	0.14	0.15	0.44	0.45	0.44	0.44	0.28	0.46
FATP21	0.21	0.20	0.54	0.56	0.54	0.53	0.35	0.52
GLUC8	0.10	0.12	0.03	0.04	0.08	0.09	0.11	0.15
GLUC19	0.01	0.10	0.03	0.05	0.04	0.05	-0.05	0.11
TRGL8	0.08	0.11	0.06	0.08	0.07	0.06	0.05	0.06
TRGL19	0.15	0.13	0.17	0.19	0.17	0.18	0.12	0.19

786 ¹For a description of the traits, see Table 1.

787 ²For a description of the models, see Table 2.

788

789 **Table 5.** Pearson's coefficient correlation (ρ) between model's components (\hat{g} , \hat{t} , \hat{t}_c and \hat{gt}) solutions and corrected phenotypes (y^*) for BLUP
790 models proposed¹. Numbers in bold (per row) show the best values for the accuracy of GEBV ($\rho_{\hat{g}-y^*}$) across models, identical results between
791 two or more models are indicated in underline.

Trait ²	Model ³											
	GTBLUP			GTIBLUP				GTCBLUP			GBLUP	
	$\rho_{\hat{g}-y^*}$	$\rho_{\hat{t}-y^*}$	$\rho_{\hat{g}-\hat{t}}$	$\rho_{\hat{g}-y^*}$	$\rho_{\hat{t}-y^*}$	$\rho_{\hat{g}-\hat{t}}$	$\rho_{\hat{g}-\hat{gt}}$	$\rho_{\hat{g}-y^*}$	$\rho_{\hat{t}_c-y^*}$	$\rho_{\hat{g}-\hat{t}_c}$	$\rho_{\hat{g}-y^*}$	
BMD12	<u>0.20</u>	0.24	0.22	<u>0.20</u>	0.22	0.21	-0.04	0.06	<u>0.20</u>	0.04	-0.10	0.19
BMD21	0.29	0.38	0.28	0.30	0.37	0.29	0.04	-0.03	0.31	0.08	-0.03	0.29
BW10	0.18	0.46	0.27	<u>0.19</u>	0.47	0.27	0.04	0.02	<u>0.19</u>	0.03	-0.13	0.18
BW15	0.15	0.52	0.29	0.15	0.51	0.28	0.02	-0.02	0.18	0.08	-0.06	0.15
BW20	0.17	0.61	0.25	0.17	0.60	0.26	-0.09	-0.02	0.21	0.16	-0.10	0.18
CHOL8	0.14	0.13	0.16	0.14	0.13	0.15	0.18	-0.01	0.15	0.04	-0.08	0.14
CHOL19	0.24	0.14	0.16	0.25	0.12	0.15	0.18	-0.02	0.27	-0.08	-0.09	0.25
FATP12	0.18	0.43	0.14	0.18	0.42	0.13	-0.03	-0.12	0.20	0.15	-0.05	0.16
FATP21	0.22	0.52	0.16	0.22	0.53	0.16	-0.09	-0.10	0.26	0.16	-0.10	0.21
GLUC8	<u>0.12</u>	0.02	0.22	<u>0.12</u>	0.01	0.20	0.02	0.06	0.11	0.04	-0.09	0.10
GLUC19	<u>0.01</u>	0.04	0.19	<u>0.01</u>	0.02	0.18	-0.04	0.05	<u>0.01</u>	-0.05	-0.11	<u>0.01</u>
TRGL8	0.08	0.05	0.16	<u>0.09</u>	0.05	0.15	0.04	0.03	<u>0.09</u>	-0.07	-0.07	0.08
TRGL19	0.14	0.15	0.15	0.14	0.15	0.14	0.03	-0.05	0.17	0.03	-0.09	0.15

792 ¹ $\rho_{\hat{g}-y^*}$ = correlation between additive genetic effect and corrected phenotypes; $\rho_{\hat{t}-y^*}$ = correlation between gene transcripts effect and corrected phenotypes; $\rho_{\hat{g}-\hat{t}}$ =
793 correlation between the additive genetic and gene transcripts effects; $\rho_{\hat{g}-\hat{gt}}$ = correlation between the additive genetic effect and the interaction between genetic and gene
794 transcript effects; $\rho_{\hat{t}-\hat{gt}}$ = correlation between the additive genetic effect and the interaction between genetic and gene transcript effects; $\rho_{\hat{t}_c-y^*}$ = correlation between gene
795 transcripts conditioned on SNP genotypes and corrected phenotypes; $\rho_{\hat{g}-\hat{t}_c}$ = correlation between the additive genetic effect and gene transcripts conditioned on SNP
796 genotypes.

797 ²For a description of the traits, see Table 1.

798 ³For a description of the models, see Table 2.

799 **Figure 1.** Percentage of variance explained by SNP genotypes (g^2), gene transcripts (t^2), the
800 interaction between them (gt^2) and not explained (e^2) by GBLUP, TBLUP, GTBLUP,
801 GTIBLUP and GTCBLUP models tested for the traits BW and FATP.

802 ¹For a description of the traits, see Table 1.

803 ²For a description of the models, see Table 2.

804

805

806 **Figure 2.** Percentage of variance explained by SNP genotypes (g^2), gene transcripts (t^2), the
807 interaction between them (gt^2) and not explained (e^2) by GBLUP, TBLUP, GTBLUP,
808 GTIBLUP and GTCBLUP models tested for the traits BMD, CHOL, GLUC and TRGL.

809

810 ¹For a description of the traits, see Table 1.

811 ²For a description of the models, see Table 2.

812

813 **SUPPLEMENTARY MATERIAL**

814

815 **Table S1.** Regression coefficient of the corrected phenotypes on prediction for validation
816 animals from all models tested. Values closer to 1 indicate less bias.

Trait ¹	Model ²							
	Only SNP ²		Only gene transcripts ²		SNP + gene transcripts ²			
	GBLUP	GGBM	TBLUP	TGBM	GTBLUP	GTIBLUP	GTCBLUP	GTGBM
BMD12	1.16	1.48	1.52	1.36	1.47	1.63	0.88	1.23
BMD21	1.47	1.82	1.67	1.34	1.65	1.95	1.13	1.21
BW10	1.07	1.46	1.25	1.46	1.28	1.44	0.85	1.16
BW15	0.80	1.82	1.08	1.44	1.06	1.17	0.70	1.12
BW20	1.01	1.82	1.09	1.36	1.09	1.16	0.82	1.07
CHOL8	1.17	1.78	0.92	1.31	1.05	1.06	0.76	0.79
CHOL19	0.99	0.79	0.79	1.43	0.92	1.00	0.83	0.69
FATP12	0.55	0.76	0.96	1.16	0.99	1.09	0.89	1.18
FATP21	1.10	0.83	1.02	1.25	1.04	1.12	0.99	1.14
GLUC8	0.38	0.44	0.29	1.27	0.31	0.31	0.68	0.52
GLUC19	0.35	1.82	0.33	1.28	0.36	0.37	0.26	0.45
TRGL8	0.54	0.61	0.36	1.83	0.37	0.36	0.58	0.86
TRGL19	0.96	1.12	0.75	1.15	0.74	0.85	0.72	1.23
Mean	0.89	1.27	0.93	1.36	0.95	1.04	0.79	0.97
Min	0.35	0.44	0.29	1.15	0.31	0.31	0.26	0.45
Max	1.47	1.82	1.67	1.83	1.65	1.95	1.13	1.23

817 ¹For a description of the traits, see Table 1.

818 ²For a description of the models, see Table 2.

819

820 **Table S2.** Relative root-mean squared error (RRMSE) for predictions on the validation set.
 821 Lower values indicate lower prediction error.

Trait ¹	Model ²							
	Only SNP		Only gene transcripts		SNP + gene transcripts			
	GBLUP	GGBM	TBLUP	TGBM	GTBLUP	GTIBLUP	GTCBLUP	GTGBM
BMD12	1.00	1.02	0.99	1.02	0.98	0.99	1.01	0.99
BMD21	0.99	1.02	0.96	0.99	0.95	0.96	0.98	0.96
BW10	0.88	0.90	0.85	0.87	0.85	0.85	0.88	0.85
BW15	0.86	0.86	0.85	0.85	0.86	0.86	0.87	0.86
BW20	0.87	0.88	0.84	0.86	0.84	0.84	0.87	0.84
CHOL8	0.89	0.90	0.89	0.91	0.89	0.89	0.90	0.87
CHOL19	0.95	0.97	0.96	0.97	0.95	0.95	0.96	0.95
FATP12	0.91	0.91	0.86	0.87	0.86	0.86	0.89	0.87
FATP21	0.85	0.87	0.77	0.78	0.77	0.77	0.81	0.77
GLUC8	1.15	1.15	1.17	1.14	1.15	1.15	1.15	1.15
GLUC19	1.31	1.27	1.33	1.27	1.31	1.31	1.34	1.31
TRGL8	1.07	1.09	1.14	1.14	1.11	1.10	1.13	1.10
TRGL19	1.19	1.22	1.18	1.16	1.18	1.17	1.20	1.21
Mean	0.99	1.00	0.98	0.99	0.98	0.98	1.00	0.98
Min	0.85	0.86	0.77	0.78	0.77	0.77	0.81	0.77
Max	1.31	1.27	1.33	1.27	1.31	1.31	1.34	1.31

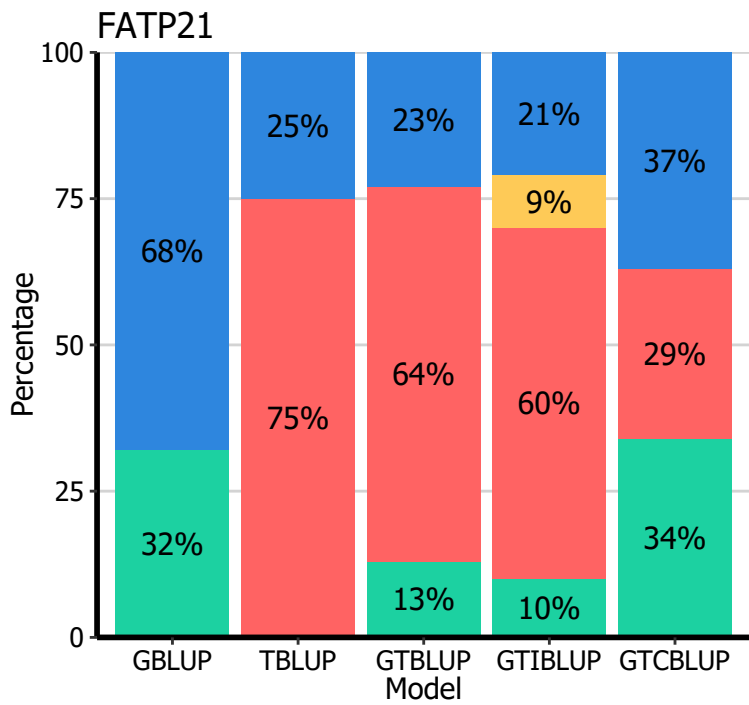
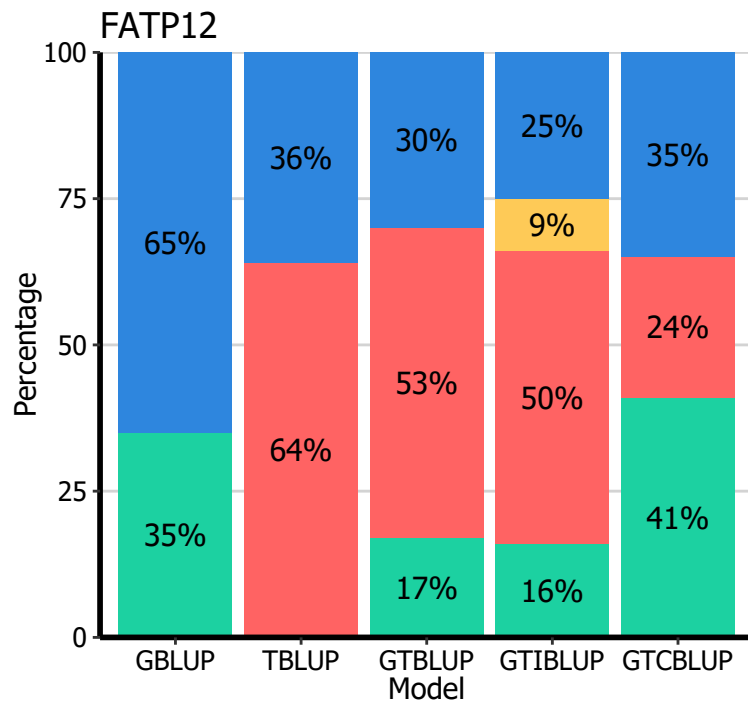
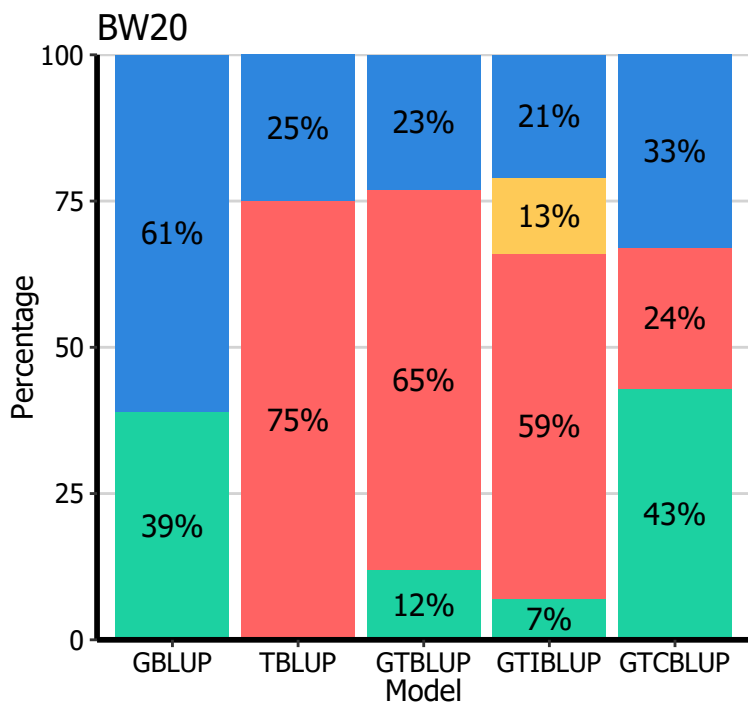
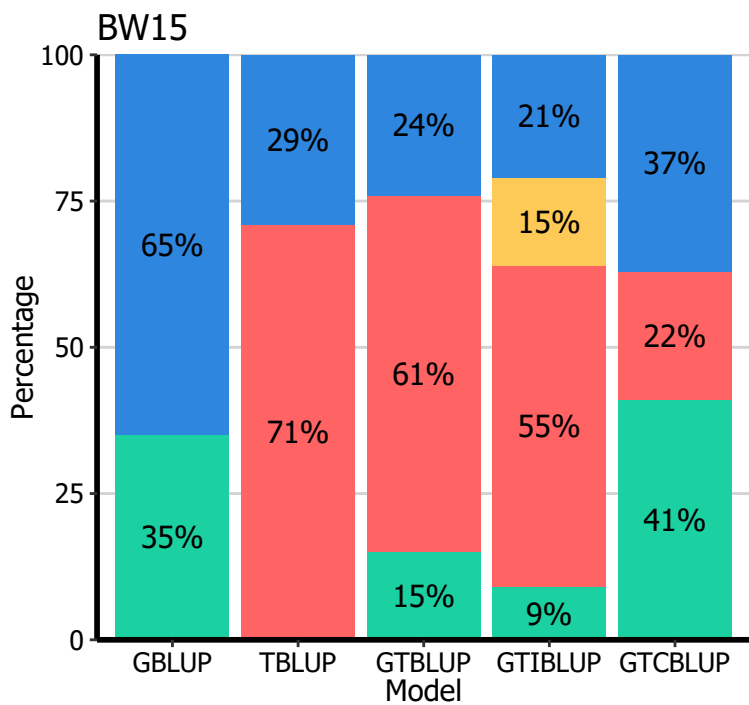
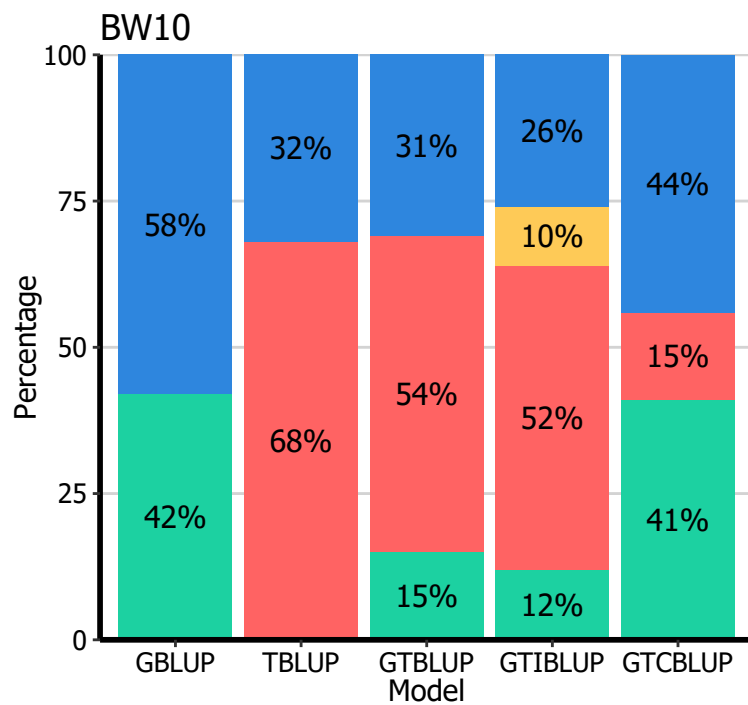
822 ¹For a description of the traits, see Table 1.
 823 ²For a description of the models, see Table 2.
 824

825 **Table S3.** Estimates of model parameters for the CORE-GREML model: the percentage of
 826 variance explained by SNP genotypes (g^2) and gene transcripts (t^2), the estimated
 827 correlation between g and t components (ρ_{gt}), p-values for the estimated correlation ($p[\rho_{gt}]$)
 828 and p-values for the likelihood ratio tests to determine whether the model fit by CORE-
 829 GREML was better than that by the standard model not including a covariance component
 830 ($p[LKH]$).

Trait ¹	CORE-GREML parameters				GREML vs CORE-GREML		
	g^2	t^2	ρ_{gt}	$p[\rho_{gt}]$	GREML	CORE-GREML	$p[LKH]$
BMD12	0.24	0.20	+0.21	0.62	-181.4712	-181.4062	0.71
BMD21	0.28	0.26	+0.14	0.55	-177.2119	-177.1537	0.60
BW10	0.04	0.40	+0.58	0.29	-695.5398	-695.3162	0.50
BW15	0.03	0.45	+0.60	0.45	-696.1394	-696.7851	0.25
BW20	0.01	0.60	+0.63	0.32	-679.8870	-680.7453	0.19
CHOL8	0.27	0.13	+0.55	0.45	-483.6665	-483.9623	0.44
CHOL19	0.21	0.18	+0.71	0.07	-388.3944	-389.8146	0.09
FATP12	0.17	0.73	-0.23	0.50	-17.1618	-17.0426	0.62
FATP21	0.08	0.89	-0.47	0.34	-3.5900	-3.4460	0.59
GLUC8	0.21	0.09	-0.22	0.76	-510.4316	-510.4436	0.87
GLUC19	0.02	0.15	-0.26	0.72	-402.9910	-403.0818	0.67
TRGL8	0.08	0.14	+0.26	0.23	-226.2193	-226.9104	0.25
TRGL19	0.09	0.25	+0.07	0.90	-171.9591	-171.9595	0.97

831 ¹For a description of the traits, see Table 1.
 832

833



e2 gt2 t2 h2

